PERIODICO di MINERALOGIA
established in 1930

Dipartimento
di Scienze della Terra
Sapienza
Università di Roma

An International Journal of
Mineralogy, Crystallography, Geochemistry,
Ore Deposits, Petrology, Volcanology
and applied topics on Environment, Archaeometry and Cultural Heritage

Chemical beneficiation of two Turkish lignites with various chemical treatments

Jale Gülen [1], Aylin Boztepe [1], Bilal Öztürk [1], Mustafa Kaya [2], Mustafa Kumral [2]

[1] Yıldız Technical University, Chemical Engineering Department, 34210 Esenler - Istanbul, Turkey
[2] Istanbul Technical University, Geological Engineering Department, 34469 Maslak-Istanbul, Turkey

ARTICLE INFO

Submitted: October 2019
Accepted: February 2020
Available on line: April 2020

* Corresponding author:
gulenj@yildiz.edu.tr

DOI: 10.2451/2020PM16606

How to cite this article:
Gülen J. et al. (2020)
Period. Mineral. 89, 135-143

ABSTRACT

In this study, Çan and Nallıhan lignites were treated with selected chemicals after hydrogen peroxide oxidation. The chemicals were methanol and acetic acid and the results discussed from the points of temperature and concemtration effects. For concentration effect, the peroxide concentration was kept as 10% and the chemicals were applied for 10, 15, and 20% concentrations. For temperature effect, all the chemicals were selected as 10 % concentration and the experiments were performed at 35, 45 and 55 ºC temperatures. 20% acetic at 55 ºC was given the best sulfur removal. FT-IR and XRD spectra of all the samples were also evaluated.

Keywords: chemicals; lignite; sulfur, FTIR, X-RD.

INTRODUCTION

Coal, shale, oil or natural gas are various forms of fossil fuels (Akkoca and Işık, 2018). Coal is a highly heterogeneous solid source originating from plants. It contains various elements combined to minerals as inorganic coal constituents. The organic structure consists mainly carbon and hydrogen and other elements like oxygen, nitrogen and sulfur (Meyers, 1977). Responsible and clean use of coal is of great importance for balancing economic development with environmental protection (Lin et al, 2018). The coals of having high sulfur constituent are unsuitable for several processes (Shang et al 2018).

The chemicals are very effective for removing all sulfur groups. Many studies are found related to the usage of alkalis like sodium carbonate (Wheelock, 1981), alkali oxidation (Lin et al., 2008), hydrogen peroxide plus sulfuric acid (Vasilokos and Clinton, 1984), ozone (Wang et al., 1987), linseed oil (Ken et al., 2019) and other chemicals like H_2O_2 (Levent et al., 2007), H_2O_2/acetic anhydride (Wang et al., 2015), stepwise demineralization (Yaman et al., 2001), microwave/(H_{Ac}-H_2O_2 effect) (Yang et al., 2016), H_2O_2/H_2SO_4 effect (Karaca and Ceylan, 1977), pyrite flotation (Zhao et al., 2019), etc. There are also several papers related to chemical treatments under ultrasonic effect. Barma et al studied the chemical beneficiation of high ash Indian noncoking coals by alkali plus acid treatmants under ultasonic effect. They reached the maximum ash removal (73.91% demineralization) with the combination effect of NaOH followed by 30% H_2SO_4 application. They optimized the study from the points of optimum chemical treatment, time and energy (Barma et al., 2018a). Barma et al studied the demineralization of low grade coal under the ultrasonic effect after HCl treatment. The results were supported by using different techniques such as X-ray diffraction (XRD), Fourier transform infrared (FTIR) spectroscopy, Raman spectroscopy, Scanning electron microscopy (SEM) and thermal gravimetric analysis (TGA). Maximum demineralization (41.28%) and desulfurization (52.17%) amounts were achieved using the ultrasonic leaching at the derived optimum conditions: coal size (+75-45) µm,, HCl concentration=1.5 M and leaching time 1.5 h (Barma et al, 2018b). Other various ultrasonic assisted applications were also given by Barma (2019).

Among these chemicals, hydrogen peroxide (H_2O_2) has a more positive oxidation potential for the pyrite and other SO_2/S couples (Meyers, 1977).

The predominant reactions (Barma, 2019):

$$H_2O_2 \rightarrow OH^- + OH^- \quad (1)$$

The product species such as OH^- radicals and H_2O_2 are highly reactive with the strong oxidation potential of 2.8 and 1.8 V, respectively, and can potentially induce oxidation of the sulfur components. For instance, H_2O_2 may oxidize sulfide at different pH values as per the reactions (Ambedkar et al, 2011):

$$H_2S + H_2O_2 \rightarrow S + 2H_2O \text{ (acidic pH)} \quad (2)$$
$$HS^- + 4H_2O_2 \rightarrow SO_4^{2-} + 4H_2O + H^+ \text{ (neutral pH)} \quad (3)$$
$$S^{2-} + 4H_2O_2 \rightarrow SO_4^{2-} + 4H_2O \text{ (alkaline pH)} \quad (4)$$

So, peroxide as the oxidising agent can give the reductions on the coal sample shown below (Meyers, 1977).

$$3FeS_2 + 3H_2O_2 \rightarrow Fe_2O_3 + 4S + 3H_2O \quad (5)$$
$$4\,S + 12\,H_2O_2 \rightarrow 4H_2SO_4 + 8\,H_2O \quad (6)$$

Tang et al. studied the action mechanism of hydrogen peroxide for coal desulfurization (Tang et al., 2018). Wang et al. have studied the effects of four ionic liquids combining with 30% H_2O_2 on the desulfurization degree of coal and the solutions were removed the organic sulfur up to 16.26%, much higher than 2.44% by single 30% H_2O_2 treatment (Wang et al., 2019).

In this study, the effects of aqueous H_2O_2 plus methanol or acetic acid have been investigated from the point of one of undesired constituents of sulfur in lignites. The concentration and temperature effects were also discussed.

EXPERIMENTAL

Nallıhan and Çan lignites were supplied from Ankara and Çanakkale cities where are in central asia and Aegean regions of Turkey.

Aqueous H_2O_2 was chosen as an oxidative medium for experimental samples. At the beginning, the sample was grounded and sieved to pass 250 µm. 3 g sample was stirred with 50 mL 10% H_2O_2 for 20 minutes at 35 °C. Then the samples was filtered, washed with distilled water and dried in the autoclave at 105 °C (NÜVE FN 055 brand). Later, it was stirred with 50 mL aqueous methanol (M) or acetic acid (A) solutions for 20 minutes. The experiments were performed from the points of concentration or temperature effects. For concentration (C) effect, the chemicals (methanol and acetic acid symbolised as MC and AC) were chosen and applied as 10, 15 and 20% concentration. For temperature (T) effect, the experiments were performed at 35, 45 and 55 °C temperatures with aquatic methanol and acetic acid solutions symbolised as MT and AT. For those experiments, the concentrations of all chemicals were kept constant as 10%. Then, the solution was filtered through the blue ribbon filter, washed with distilled water and dried in the autoclave at 105 °C. The sulfur in ash, burnable sulfur values and calorific values were recorded from U therm YX-GY model analyzer and U therm YX ZRA model calorimeter, respectively. The sulfur analyses of the demineralized samples were done according to ASTM standards (ASTM D 2492, 1983).

RESULTS AND DISCUSSION

Concentration effect

The proximate analysis of the two lignites was seen in Table 1. The sulfur amounts of Nallıhan and Çan lignites were 6.66% and 3.85%, respectively. The concentration and temperature effects were discussed from the sulfur removals that one of the undesired constituent of lignite.

The possible interactions of the samples with the chemicals are shown in the following Tables 2 and 3.

MC and AC effects were shown on the Table 4. Total sulfur values were decreased to 4. 47 and 2.44 for Nallıhan being treated with 20% MC and AC, respectively. Similarly, total sulfur values were obtained as 2.35 and 2.20 for Çan lignite with 20% MC and AC applications. With 20% MC treatment, maximum 33% sulfur removal was leached from Nallıhan lignite. This ratio reached to 39% for Çan lignite (The values in parantheses). Those

Table 1. Proximate analysis (%) of Çan and Nallıhan lignites.

Lignite	Fixed carbon	Volatile matter	Sulfur	Ash	Moisture	Calorific value (kJ/kg)
Nallıhan	54.09	20.28	6.66	14.51	11.12	4869
Çan	54.06	30.08	3.85	5.16	10.70	5354

Table 2. Methanol and lignite interactions.

Lignite	Chemical	Reactions involved
Nallıhan	Methanol	$FeS_2 \rightarrow Fe_2O_3$ ($FeO.FeO_2$ other reactions Si, Ca, clay minerals)
Çan	Methanol	$FeS_2 \rightarrow Fe_2O_3$ ($FeO.FeO_2$ other reactions Si, Ca, clay minerals)

Table 3. Acetic acid and lignite interactions.

Lignite	Chemical	Reactions involved
Nallıhan	Asetic acid	$FeS_2 \rightarrow Fe_2O_3$ ($FeO.FeO_2$ other reactions Si, Ca, clay minerals)
Çan	Asetic acid	$FeS_2 \rightarrow Fe_2O_3$ ($FeO.FeO_2$ other reactions Si, Ca, clay minerals)

Table 4. The sulfur values of the lignites after chemicals treatments (The parantheses show the percent removals).

Lignite	MC effect			AC effect		
	10%	15%	20%	10%	15%	20%
Nallıhan	5.36	5.01	4.47	5.10	4.93	2.44
	(19.52)	(24.77)	(32.88)	(23.42)	(25.98)	(63.36)
Çan	3.37	2.98	2.35	3.30	2.40	2.20
	(12.47)	(22.60)	(38.96)	(14.29)	(37.66)	(42.86)

removals were found as 63% and 43% for Nallıhan and Çan lignites with 20% aqueous AC solutions, respectively. AC was more effective for removing the sulfur amount and given the best result for Nallıhan lignite. This may be due to the separate pyrite particle groups (Gülen, 2007).

$CH_3^+OH^-$ and $CH_3COO^-H^+$ radicals can give various chemical bonds with lignite during the experiment. It is the possible pathways of the chemicals with lignite (Li et al., 2015)(Figure 1, Li et al., 2015).

Detailed proximate analysis was also given in Table 5 and 7 for Nallıhan and Çan lignites, respectively. The values of sulfur in ash and burnable sulfur of chemicals treated samples were also given for Nallıhan and Çan lignites. The volatile matters of Nallıhan lignite were raised to 35.30% and 34.76% and the ash values were decreased to 11.13% and 10.85% for Nallıhan lignite being treated with 20% MC and AC. Those effects were also decreased the sulfur in ash and burnable sulfur amounts of Nallıhan lignite (Table 5).

Similarly, the volatile matter of Çan lignite were increased to 45.35% and 44.78% and ash values were decreased to 5.16 and 4.59 for Çan lignite with 20% MC and AC treatments (Table 7). The sulfur in ash and burnable sulfur amounts for 20% MC and AC treated Çan lignite were found as 0.10; 0.11 and 1.23; 1.33, respectively (Table 7). Gülen et al. have studied the effects of concentration variation of acids and alkalis on the Turkish coals (Gülen et al., 2005). Demirbaş reached rather successful removals on demineralization and desulfurization degree of coals via column froth flotation and he also compared the various methods each other (Demirbaş, 2002).

Temperature effect

The temperature effects were also discussed from % sulfur removals on the Nallıhan and Çan lignites. The sulfur variation and the % sulfur removal were given in Table 6 for Nallıhan and Çan lignites, respectively.

Total sulfur values were found as 3.06 and 1.11 for Nallıhan lignite at 55 °C with 10% MT and AT solutions. The sulfur values were decreased to 2.20 and 2.65 for Çan lignite with 10% MT and AT at 55 °C, respectively (Table 6). With MT at 55 °C, maximum 54% sulfur removal was leached in Nallıhan lignite as seen from Table 6. This removal raised to 83% with AT treatment at 55 °C. Those values were found as 43% and 31% for Çan lignite at 55 °C, respectively (Table 6). The acetic acid is more effective than methanol in Nallıhan lignite. The acidic medium was rather effective on the sulfur removal of lignite (Ambedkar, 2011). Ward applied (Ward, 1974) hydrogen peroxide washing on coal at various temperatures. Temperature has shown rather drastic effects on the chemical procedure.

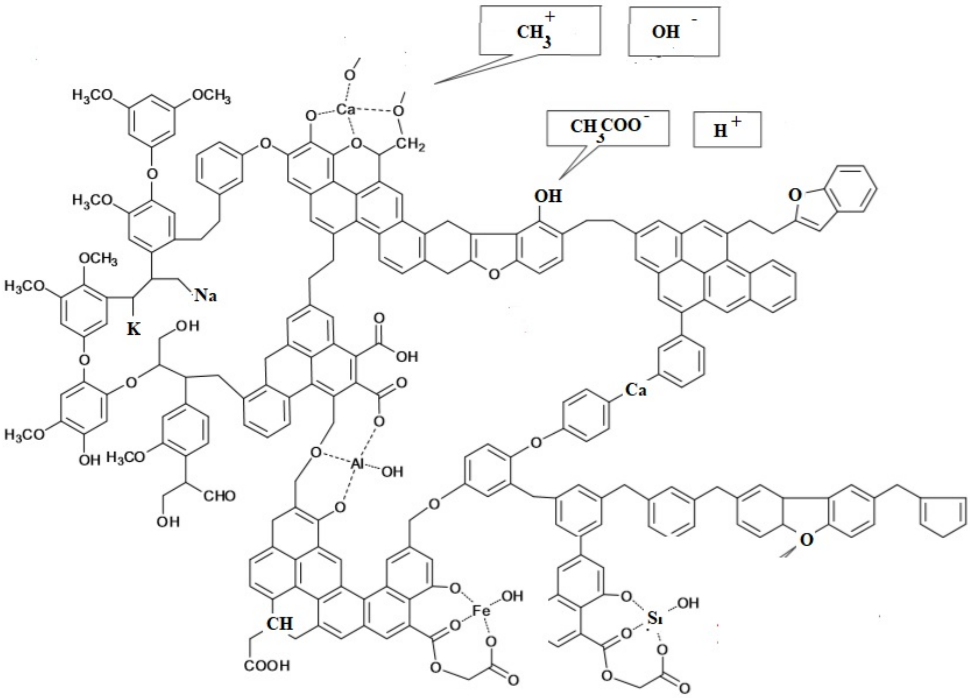

Figure 1. Possible pathways of chemicals with lignite.

Table 5. The results of Nallıhan lignites at the optimum conditions.

	Original	MC 20%	AC 20%	MT 55 °C	AT 55 °C
Moisture	11.12	11.12	11.12	11.12	11.12
Ash	14.51	11.13	10.85	11.90	11.15
Volatile Matter	20.28	35.30	34.76	36.40	35.45
Fixed Carbon	54.09	42.45	43.27	40.58	42.28
Total	100	100	100	100	100
Total Sulfur	6.66	5.41	5.00	5.11	5.41
Sulfur in Ash	0.56	0.30	0.25	0.40	0.33
Burnable Sulfur	6.10	5.11	4.75	4.71	5.08
Low Heating Value (Kcal/kg)	3340	4146	4071	4224	4154

Table 6. The sulfur % of the lignites at various temperatures (The parantheses show the percent removals).

Lignite	MT effect			AT effect		
	35 °C	45 °C	55 °C	35 °C	45 °C	55 °C
Nallıhan	3.37	3.21	3.06	3.10	1.83	1.11
(49.40)	(51.80)	(54.05)	(53.45)	(72.52)	(83.33)	
Çan	2.75	2.40	2.20	2.79	2.74	2.65
(28.57)	(37.66)	(42.86)	(27.53)	(28.83)	(31.17)	

Table 7. The results of Çan lignites at the optimum conditions.

	Original	MC 20%	AC 20%	MT 55 °C	AT 55 °C
Moisture	10.70	10.70	10.70	10.70	10.70
Ash	5.75	5.16	4.59	5. 00	4.85
Volatile Matter	29.49	45.35	44.78	46.85	45.69
Fixed Carbon	54.06	38.79	39.93	37.45	38.76
Total	100	100	100	100	100
Total Sulfur	3.85	1.33	1.44	1.56	1.63
Sulfur in Ash	0.12	0.10	0.11	0.12	0.12
Burnable Sulfur.	3.73	1.23	1.33	1.43	2.15
Low Heating Value (Kcal/kg)	3340	4753	4838	4685	4793

The values of sulfur in ash, burnable sulfur and low heating values can also be seen from Table 5 and 7 for Nallıhan and Çan lignite while the temperature augmentation was affected. The ash values for Nallıhan lignite were found as 11.90 and 11.15 with MT and AT effects at 55 °C (Table 5). Those values were recorded as 5.00 and 4.85 for Çan lignite (Table 7). The volatile matter for Nallıhan lignite were 36.40 and 35.45 as shown in Table 5. The similar values were detected as 46.85 and 45.69% for Çan lignite with MT and AT effects at 55 °C as seen in Table 7. The temperature variation gives better results than concentration variation of chemicals for Nallıhan lignite that is shown in Table 6. Dash et al., have showed the positive effects of the elevated temperature and pressure on the leaching characteristics of Indian coals (Dash et al., 2015). Gülen et al have several papers related to the various effects from the points of undesired constituents of the coals (Doymaz et al., 2007; Gülen et al., 2013).

FTIR SPECTRA

a) Nallıhan lignite

The FTIR spectra of the Nallıhan lignite and other chemical treated samples were shown in Figure 2. The spectra were recorded in the region between 4000-400 cm^{-1} with Perkin Elmer spectrophotometer by Attenuated Total Reflectance (ATR) technique. The bottom spectrum represents Nallıhan lignite (a). The others are Nallıhan AT(55°C) (b), Nallıhan AC(20%) (c), Nallıhan MT(55 °C) (d) and Nallıhan MC(20%) (e) from bottom to up, respectively. Nallıhan lignite gives peaks at 469, 600 and 664 cm^{-1} due to the mineral matter. The band seen at 1120 cm^{-1} is originated due to the S=O stretching (Li et al., 2019). The peak seen at 1135 cm^{-1} show C-H stretching. There are two small peaks at 1396, 1432 cm^{-1} and a broad peak at 1618 cm^{-1} that were the indicator of C=C and C=O vibrations. The peak seen at 3384 cm^{-1} is represented

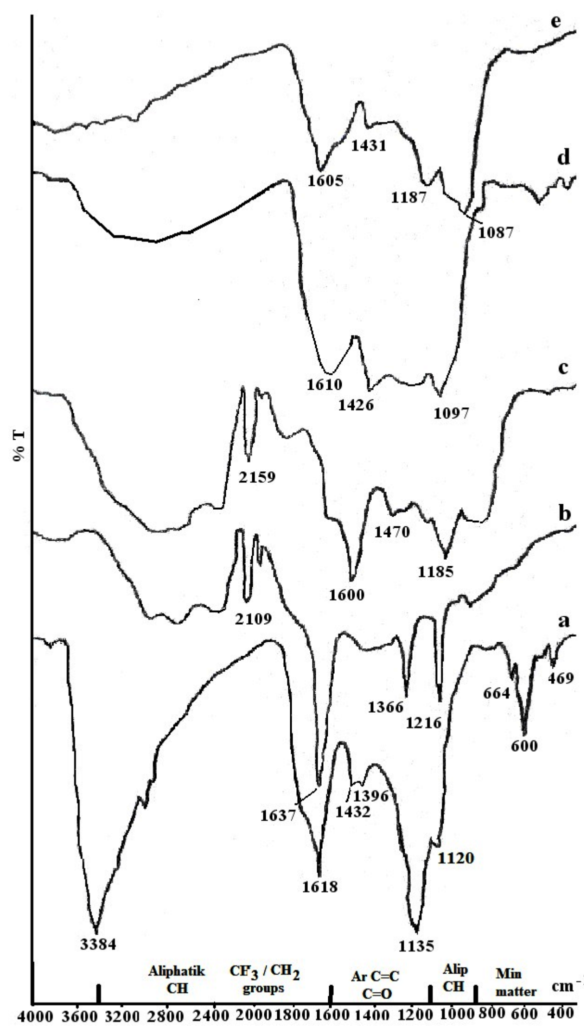

Figure 2. FTIR spectra of Nallıhan lignite: (a) original, (b) Nallıhan AT sample, (c) Nallıhan AC sample, (d) Nallıhan MT sample, (e) Nallıhan MC sample.

aliphatic C-H groups. Clay minerals usually have given absorption beyond 3500 cm^{-1} of the FT-IR spectrum.

With acetic acid treatment (b, c), the mineral matter of the coal is removed. The peak intensities are decreased at 1216, 1366 and 1637 cm^{-1} for (b) and 1185, 1470 and 1600 cm^{-1} for (c)plot. Those peaks show C-H stretching, etheric oxygen groups and aromatic C=C and C=O stretching, respectively. The similar peaks are seen at 1097, 1187, 1426 and 1610 cm^{-1} for (d) and 1087, 1431 and 1605 cm^{-1} for (e) plot. The band showing C-H group at 3384 cm^{-1} of original sample (a) was rounded for all plots (b, c, d, e).

b) Çan lignite

Figure 3 shows the FTIR spectra of Çan and other chemical treated lignites. The bottom spectrum represents original Çan lignite(a). The samples are sequenced from bottom to top as (a) Çan lignite, (b) Çan AT(55 °C), (c) Çan AC(20%), (d) Çan MT(55 °C), (e) Çan MC(20%) from bottom to top, respectively. The peaks seen at 473, 536, 598 and 801 cm^{-1} are the evidence of the mineral matter existence. The absorption pattern in this region is frequently complex with the bands originating in interacting vibrational modes. Both organic and inorganic constituents may exist in this region. The peaks seen at 1033, 1096 and 1262 cm^{-1} are due to C-O stretching. The

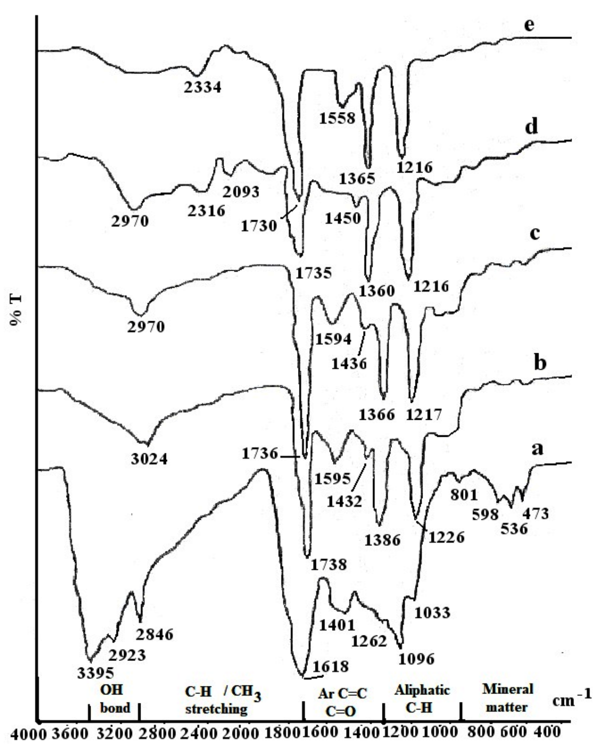

Figure 3. FTIR spectra of Çan lignite (The plots are defined below): (a) original, (b) Çan AT sample, (c) Çan AC sample, (d) Çan MT sample, (e) Çan MC sample.

1033 cm^{-1} peak also shows S=O stretching (Li et al., 2019). Etheric oxygen group gives a small shoulder at 1401 cm^{-1}. The peak at 1618 cm^{-1} is the indicator of an aromatic C=C and C=O stretching. Aliphatic C-H groups and CH_3 stretching give absorbances at 2846 cm^{-1} and 2923 cm^{-1}. The peak seen at 3395 cm^{-1} is due to O-H stretching.

With peroxide plus acetic acid effect (b, c), the mineral groups of Çan lignite are removed. The sharp peaks are seen at 1226 and 1386 cm^{-1} for (b) plot. Those peaks give absorbances at 1217 and 1366 cm^{-1} for (c) plot. The similar peaks are found for (d) and (e) plots at 1216, 1360 cm^{-1} and 1216, 1365 cm^{-1} which are seen due to C-H stretching and C=C or C=O stretching, respectively. The organic structure is given peaks at 1432 and 1595 cm^{-1} for (b) and 1436 and 1594 cm^{-1} for (c) plots due to C=C or C=O stretching. The similar peaks have seen at 1450 and 1558 cm^{-1} for (d) and (e), respectively. The peak seen at 1618 cm^{-1} in original sample (a) turns into narrow and sharp peaks for other Çan chemical treated plots at 1738, 1736, 1735 and 1730 cm^{-1} for (b, c, d) and (e), respectively. This may be the result of mineral matter removal and consequently, the increase of concentration of the organic part. The peak that shows O-H stretching at 3395 cm^{-1} for original sample are rounded for (b) and (c) plots at 3024 and 2970 cm^{-1} wave numbers. But, the peaks seen at 2093, 2316 and 2970 cm^{-1} are the indicator of the C-H stretching and CH_3/CH_2 groups for (d) plot, respectively. This peak gives absorbance at 2334 cm^{-1} wave number for (e) plot.

X-RD ANALYSIS

a) Nallıhan Lignite

XRD diffractions were obtained in a Bruker D8 Advance model X-Ray diffractometer. Diffraction patterns were collected at 0º-90º 2Θ using Cu Kα radiation. Sample preparation and instrumental conditions were identical for all specimens. The mineral groups of lignites that could not be removed with chemical treatments were characterized by X-RD diffractograms.

The bottom plot represents the original Nallıhan lignite in Figure 4. The others are sequenced Nallıhan AT (55 °C), Nallıhan AC(20%), Nallıhan MT(55 °C) and Nallıhan MC(20%) from bottom to top, respectively.

Some mineral groups such as quartz, anhydrite, hematite and feldspar were found in Nallıhan lignite according to the X-Ray diffractions. It can be deduced the major mineral species of the original Nallıhan lignite consisted of quartz (SiO_2) (2Θ=9.820, 11.648, 20.736 and 29.107), hematite (Fe_2O_3) (2Θ=17.643, 22.239, 22.383, 22.665, 28.654, 31.092 and 33.365), pyrite (FeS_2) (30.111, 33.105) and feldspar Na-K($AlSi_3O_8$)/Ca($AlSi_3O_8$) (clay) (2Θ=23.386, 25.964, 27.763, 28.096 and 29.907), respectively. With Nallıhan AC treatment,

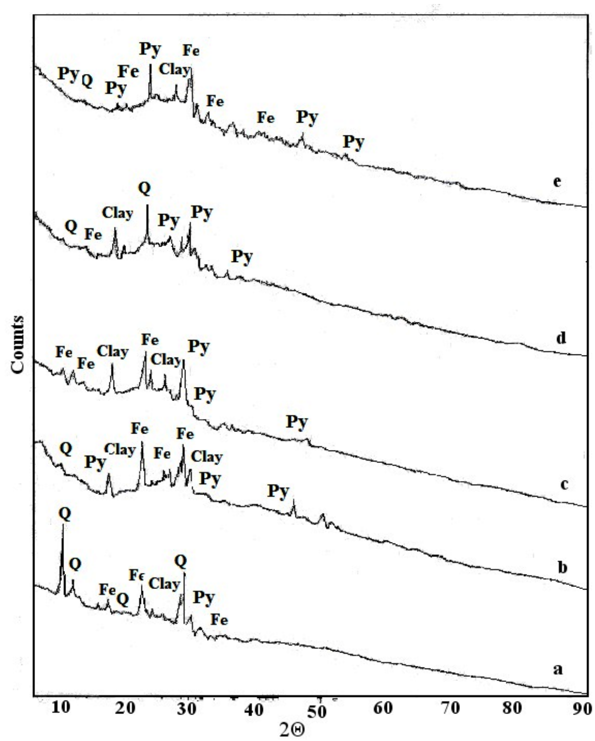

Figure 4. XRD spectra of Nallıhan lignite (a) original, (b) Nallıhan AT sample, (c) Nallıhan AC sample, (d) Nallıhan MT sample, (e) Nallıhan MC sample.

those mineral species were identified. Quartz (2Θ=9.799), hematite (2Θ=22.226, 22.406, 22.656, 28.643, and 28.975), feldspar (2Θ=11.189, 17.496, 23.607, 25.993, 26.602, 28.061, 29.531 and 19.915) and pyrite mineral groups (2Θ=18.958, 31.853, 45.748, and 49.770).

Nallıhan AT treatment, the peaks were recorded as quartz (2Θ=9.797) hematite (2Θ=22.220, 22.381, 22.631, 28.634, 28.966, and 51.418), feldspar (2Θ=17.479, 25.964, 26.637, 27.790, 28.016 and 29.847) and pyrite (2Θ=31.883, 32.560, 35.223, and 45.847).

Nallıhan MT treatment gives peaks at (2Θ=9.600) quartz; at (2Θ=25.620, 28.550 and 28.731) hematite; at (2Θ=18.409, 29.604 and 29.900) feldspar and at (2Θ=32.850, 35.560 and 39.223) pyrite groups.

Nallıhan MC treatment, those groups were seen at (2Θ= 9.847), (2Θ=22.226, 22.421, 22.662, 22.749, 28.654 and 28.980), (2Θ=17. 507, 25.984, 28.070 and 29.870), and (2Θ=11.165, 14.895, 18.999, 26.686, 31.893, 35.479, 45.816, 49.815 and 62.346) as quartz, hematite, feldspar and pyrite, respectively.

b) Çan Lignite

The bottom plot represents the original Çan lignite in Figure 5. The others are sequenced Çan AT (55 °C), Çan 20% AC, Çan MT(55 °C) and Çan 20% MC from bottom to top, respectively.

Original lignite consists of some main group like hematite, quartz and anhydride. Those groups give peaks at (2Θ=11.606, 12.486, 20.707, 26.599, 28.608, and 29.101) for hematite; at (2Θ=25.560, 38.486) for quartz (2Θ=31.743, 32.133) for pyrite and (2Θ=17.486, 24.878, 31.062, 33.305, 40.476, 45.806 and 49.701) for anhydride, respectively.

Çan AC treatment, those groups are seen at (2Θ=26.623) for quartz, (2Θ=29.878) for Clay, (2Θ=34.276, 35.434) for pyrite and (2Θ=12.319, 17.506, 20.807, 28.566, 29.600, 32.538, 45.799 and 49.834) for hematite, respectively.

Çan AT treatment, those groups were observed at (2Θ= 26.676 for quartz, (2Θ=28.878) for Clay, (2Θ=32.156, 33.434) for pyrite and (2Θ=12. 344, 17. 588, 28.705, 29.186, 32.767, 45.837 and 49.898) for hematite. Çan MT treatment, quartz and hematite groups are found at (2Θ=26.648) for quartz, and (2Θ=12.323, 17.529, 20.848, 24.986, 28.625, 29.154, 36.676, 45.787 and 49.735) for hematite respectively.

Çan MC treatment, the major peaks at (2Θ=17.204, 26.622 and 28.650 is due to quartz. The peaks at (2Θ=27.204) for Clay and (2Θ=41.204) for pyrite groups. The peaks observed at (2Θ=12. 234, 17.507, 20.837, 24.823, 29.126, 45.756 and 49.760) represent hematite group.and (2Θ=12.323, 17.529, 20.848, 24.986, 28.625, 29.154, 36.676, 45.787 and 49.735) for hematite respectively.

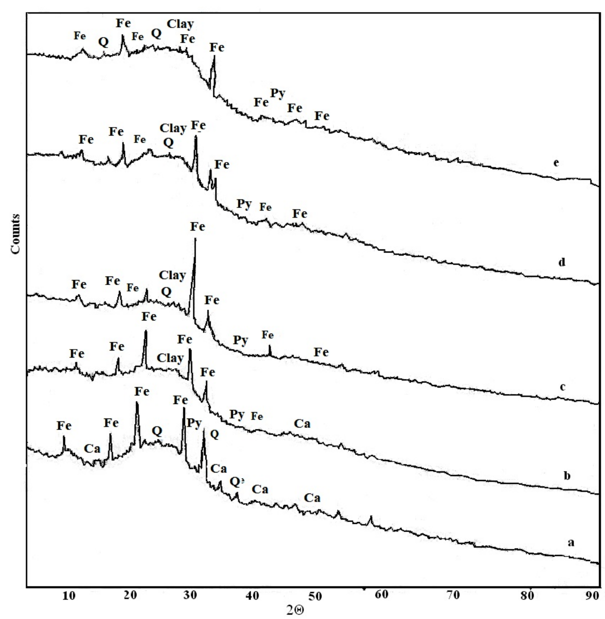

Figure 5. XRD spectra of Çan lignite (Thee plots are defined below) (a) original, (b) Çan AT sample, (c) Çan AC sample, (d) Çan MT sample, (e) Çan MC sample.

Çan MC treatment, the major peaks at (2Θ=17.204, 26.622 and 28.650) is due to quartz. The peaks at (2Θ=27.204) for Clay and (2Θ=41.204) for pyrite groups. The peaks observed at (2Θ=12.234, 17. 507, 20.837, 24.823, 29.126, 45.756 and 49.760) represent hematite group.

CONCLUSIONS

In this study, Nallıhan and Çan lignites were treated with aqueous H_2O_2 plus various chemicals like methanol or acetic acid of various concentrations and temperatures. The augmentation in temperature was more effective than concentration augmentation from the point of sulfur removal. FTIR spectra were also given for original and other chemical treated samples. The samples have organic constituents that are seen from C-H and C=O stretching vibrations. Some mineral groups such as clay types were leached from the lignites that is evidence from the FTIR spectra. X-RD analyses give detailed explanation of mineral groups of lignites.

REFERENCES

Akkoca D.B. and Işık A., 2018. Geochemistry of Paleozic Dadaş shales from the foreland of South eastern Turkey, Bismil, Diyarbakır. Periodico di Mineralogia 87, 207-225.

Ambedkar B., Nagarajan R., Jayanti S., 2011. Ultrasonic coal-wash for de-sulfurization. Ultrasonics - Sonochemistry 18, 718-726.

ASTM, 2492, 1983. American Society for Testing and Materials Annual Book of ASTM Standards Part 26: Philadelphia, PA.

Barma S.B., 2019. Ultrasonic assited coal beneficiation: A review. Ultrasonics - Sonochemistry 50, 15-35.

Barma S.D., Prasanta Sathish R., Baskey P.R., Biswal S.K., 2018a. Chemical beneficiation of high ash Indian noncoking coal by alkali leaching under low frequency ultrasonication. ACS Energy & Fuels 32, 1309-1319.

Barma S.D., Sathish R., Baskey P.K., 2018b. Ultrasonic assited cleaning of Indian low grade coal for clean and sustainable energy. Journal of cleaner production 195, 1203-1213.

Dash, P.S., Lingam R. K., Kumar S.S., Suresh P., Banarjee P.K., Ganguly S., 2015. Effect of elevated temperature and pressure on the leaching characteristics of Indian coals. Fuel 140, 302-308.

Demirbaş A., 2002. Demineralization and desulfurization of coals via column froth flotation and different methods. Energy Conversion and Management 43, 885-895.

Doymaz İ., Gülen J., Pişkin S., Toprak S., 2007. The effects of aqueous and various acid treatments on the removal of mineral matter in asphaltites. Energy Sources 29, 337-346.

Gülen J., Doymaz İ., Pişkin S., Öngen S., 2013. The effects of temperature and mineral acids on the demineralization degree of Nallıhan lignite. Energy Sources 35, 202-208.

Gülen J., 2007. Mineral matter identification in Nallıhan lignite by leaching with mineral acids. Energy Sources 29, 231-237.

Gülen J., Doymaz İ., Toprak S., Pişkin S., 2005. Removal of mineral matter from Silopi Harput asphaltite by various acid treatments. Energy Sources 27, 1457-1464.

Karaca H. and Ceylan K., 1977. Chemical cleaning of Turkish lignites by leaching with aqueous hydrogen peroxide. Fuel Processing Technology 50, 19-33.

Ken S., Kumar B., Nandi B., 2019. Desulfurization of high sülfür Indian coal by oil agglpmeration using linseed oil. Powder Technology, 34, 690-697.

Levent M., Kaya O., Kocakerim M., Yiğit V. and Küçük Ö., 2007. Optimization of desulphurization of Artvin-Yusufeli lignite with acidic hydrogen peroxide solutions. Fuel 86, 983-992.

Li H., Shi S., Lin B., Lu J., Ye Q., Lu Y., Wang Z., Hong Y., Zhu X., 2019. Effects of microwave-assisted pyrolysis on the microstructure of bituminous coals. Energy 187, article no: 115986.

Li G.Y., Ding J. X., Zhang H., Hou C.X., Wang F., Li Y.Y., Lang Y.H., 2015. ReaxFF simulations of hydrothermal treatment of lignite and its impact on chemical structures. Fuel 154, 243-251

Lin D., Qiu P., Xie X., Zhao Y., Chen G., Zeng L., 2018. Chemical structure and pyrolysis characteristics of demineralized of Zhundong coal. Energy Sources Part A 40, 282-287.

Lin K., Yang J., Jia J., Wang Y., 2008. Desulphurization of coal via low temperature atmospheric alkaline oxidation. Chemosphere 71, 183-188.

Meyers R.A., 1977. Coal desulphurization. Marcel Dekker Inc., New York.

Shang L., Li, J., Zhao Sh., Tian Y., Zhang Zh., Zhang L., 2018. Study on inytrinsic sulfidation of iron oxides and oxidation behavior of sulfidation products. Bulgarian Chemical Communications, 50, 133-140.

Tang L., Chen S., Wang S., Tao X., He H., ,Feng L., Zheng L, Ma C., Zhao Y., 2018. Exploration on the action mechanism of microwave with peroxyacetic acid in the process of coal desulfurization. Fuel 214, 554-560.

Vasilakos N.P. and Clinton C.S., 198. Chemical benefication of coal with aqueous hydrogen peroxide/sulfuric acid solutions. Fuel 63l, 1561-1563.

Wang L., Jin G., Xu Y., 2019. Desulfurizarion of coal using four ionic liquids with [HSO_4]. Fuel 236, 1181-1190.

Wang Y.G., Wei X.Y., Liu J., Yan H.L., Wei Z.H., Li Y., Li P., Liu F.J., Zong Z.M., 2015. Oxidation of Shenmu char powder with aqueous hydrogen peroxide-acetic anhydride. Fuel Processing Technology 136, 56-63.

Wang C.C., Streeter R.C., Young R.K., Shah Y.T., 1987. Kinetics of the ozonation of pyrite in aqueous solution. Fuel 66, 1574-1578.

Ward C.R., 1974. Isolation of mineral matter from Australian bituminous coals using hydrogen peroxide. Fuel. 53, 220-221.

Wheelock T.D., 1981. Oxydesulfurization of coal in alkaline solutions. Chemical Engineerig Communications 12, 137-160.

Yaman S., Yavuz R., Küçükbayrak S., Taptık Y., 2001. Stepwise demineralization and chemical isolation of the mineral matter of Göynük lignite. Energy Conversion & Management 42, 2119-2127.
Yang Y., Tao X., Kang X., He H., Yang X., Tao X,. Kang He H., Xu N., Tang L., Luo L., 2016. Oxidation of Shenmu char powder with aqueous hydrogen peroxide-acetic anhydride. Fuel Processing Technology, 143, 176-184.
Zhao K., Gu G., Yan W., Wang C., Xu L., 2019. Flotation of fine pyrite by using N-dodecyl mercaptan as collector in natural pH pulp. Journal of Materials Research and Technology 8, 1571-1575.